Quasiperiodicity route to spatiotemporal chaos in one-dimensional pattern-forming systems

Marcel G. Clerc[*] and Nicolas Verschueren

Departamento de Física, Facultad de Ciencias Físicas y Matemáticas, Universidad de Chile, Casilla 487-3, Santiago Chile
(Received 29 August 2013; revised manuscript received 4 November 2013; published 22 November 2013)

We propose a route to spatiotemporal chaos for one-dimensional stationary patterns, which is a natural extension of the quasiperiodicity route for low-dimensional chaos to extended systems. This route is studied through a universal model of pattern formation. The model exhibits a scenario where stationary patterns become spatiotemporally chaotic through two successive bifurcations. First, the pattern undergoes a subcritical Andronov-Hopf bifurcation leading to an oscillatory pattern. Subsequently, a secondary bifurcation gives rise to an oscillation with an incommensurable frequency with respect to the former one. This last bifurcation is responsible for the spatiotemporally chaotic behavior. The Lyapunov spectrum enables us to identify the complex behavior observed as spatiotemporal chaos, and also from the larger Lyapunov exponents characterize the above instabilities.

I. INTRODUCTION

Macroscopic systems maintained far from equilibrium exhibit spatially coherent structures, *patterns*, which are ubiquitous in nature [1–5]; these appear as a way to optimize energy transport [2–5]. As the parameters of the system are changed, stationary patterns can become unstable and bifurcate to more complex patterns, even into aperiodic dynamics states [5–8]. This behavior is characterized by complex spatiotemporal dynamics exhibited by the pattern and a continuous coupling between modes in time and space. Complex spatiotemporal dynamics of patterns have been observed, for example, in fluids [9–11], chemical reaction-diffusion systems [12], cardiac fibrillation [13], electroconvection [14], fluidized granular matter [15], and in a liquid crystal light valve [16]. However, the above scenario or *route* is not fully understood in the context of extended systems, since there is not a well-established qualitative theory of the partial differential equations. Several routes have been proposed for the transition from order to disorder in wave media such as defect-mediated turbulence [7], onset of space-time chaos in Galilean invariant systems [8], spatiotemporal intermittence [17], quasiperiodicity [18], crisis of spatiotemporally chaotic saddles [19], spatiotemporal chaos via stationary branching shocks and holes [20], and phase turbulence [21]. Despite the above mechanisms in wave media, the understanding of how pattern-forming systems acquire a complex spatiotemporal dynamics still has not been elucidated.

A classic scenario for the emergence of complexity in low-dimensional systems is the quasiperiodicity route [22]. By modifying a control parameter, this route shows a transition from a stationary solution to an oscillatory one through an Andronov-Hopf bifurcation. Following the parameter value modification, the solution displays a second incommensurate frequency with respect to the original one, generating a quasiperiodic behavior. Further modification of the parameter will induce the emergence of temporal chaotic behavior [22,23].

A prototype model used to explain the emergence of patterns in one-dimensional non-equilibrium systems is the Swift-Hohenberg equation, which was initially proposed in the context of Rayleigh-Bernard convection [3–5,24]. This nonlinear model accounts for the spatiotemporal evolution of a scalar field, which is an order parameter that describes the dynamics near the confluence of a spatial bifurcation and a stationary pitchfork instability with reflection symmetry. This bifurcation of codimension two in the parameter space corresponds to a *Lifshitz point* [5]. The Swift-Hohenberg equation is a variational type equation, that is, the dynamics described by this model is characterized by the minimization of a functional. Hence, the system can only exhibit stationary behaviors such as patterns and uniform states. Therefore, the appearance of permanent behaviors as oscillations, low-dimensional chaos, or spatiotemporal chaos must be ruled out from this prototype model. To account for the complex spatiotemporal dynamics observed in several optical systems, a nonvariational generalization of the Swift-Hohenberg equation has been proposed [25–28]. This model describes a Lifshitz point bifurcation without reflection symmetry. This nonvariational model has been derived in several contexts ranging from biological to nonlinear optics systems [25–28].

In this manuscript we study the route shown by a cellular pattern on its transition toward spatiotemporal chaos for the nonvariational generalization of the Swift-Hohenberg equation, which describes pattern formation in nonvariational systems. The model presents a route from stationary to spatiotemporal chaotic pattern characterized by two successive bifurcations. Initially the pattern undergoes a spatial period doubling subcritical Andronov-Hopf bifurcation, which gives rise to an oscillatory pattern. This dynamical behavior is dominated by the Andronov-Hopf frequency and its harmonics. Subsequently, a second bifurcation displays the appearance of an incommensurable frequency with respect to the former one. This last bifurcation is responsible for the spatiotemporal chaotic behavior of patterns. Using the Lyapunov spectrum we identify the most complex behavior observed as spatiotemporal chaos, and also from the larger Lyapunov exponents characterize the above instabilities. The former scenario is a natural extension of the quasiperiodicity route of low-dimensional chaos to extended systems.

The manuscript is organized as follow: In Sec. II the nonvariational generalization of the Swift-Hohenberg equation is introduced and its rich spatiotemporal dynamics is described.

---

*marcel@dfi.uchile.cl

The Lyapunov spectrum allows us to characterize the spatiotemporal chaos exhibited by the patterns. In Sec. III the route to spatiotemporal chaos of one-dimensional patterns of the nonvariational generalization of the Swift-Hohenberg equation is analyzed. In particular, the instabilities that characterize the spatiotemporal chaos route, such as the Andronov-Hopf bifurcation and the emergence of spatiotemporal chaos of pattern, are studied. Our conclusions are left to the final section.

II. ONE-DIMENSIONAL NONVARIATIONAL PATTERN FORMING MODEL

The model that describes the dynamics near the confluence of a spatial instability and a stationary bifurcation without reflection symmetry for the order parameter is *the nonvariational generalization of the Swift-Hohenberg equation* or *the Lifshitz normal form* [25,28],

$$\partial_t u(x,t) = (\eta + \epsilon u - u^3 + \nu\,\partial_{xx}u - \partial_{xxxx}u)$$
$$+ b\,u\,\partial_{xx}u + c\,(\partial_x u)^2, \qquad (1)$$

where the order parameter $u(x,t)$ is a scalar field, $\{x,t\}$ account for the space and the time coordinates, ϵ is the bifurcation parameter, η accounts for the asymmetry between homogeneous states, c is the nonlinear advection coefficient, and $\{\nu,b\}$ are, respectively, the linear and nonlinear diffusion coefficients. The linear term on the right side of Eq. (1) with fourth spatial derivative accounts for hyperdiffusion. The higher terms are eliminated by considering the following scaling: $\epsilon \ll 1$, $\partial_t \sim \epsilon$, $\eta \sim \epsilon^{3/2}$, $u \sim \epsilon^{1/2}$, $\partial_x \sim \epsilon^{1/4}$, $\nu \sim \epsilon^{1/2}$, $b \sim O(1)$, and $c \sim O(1)$. Hence, Eq. (1) is an order parameter equation describing the dynamics around Lifshitz point [29]. Notice that for $b = c = \eta = 0$ the previous model, Eq. (1), corresponds to the well-known Swift-Hohenberg equation [24]. The additional terms ($b \neq c \neq 0$) forbid the existence of a Lyapunov functional, allowing the existence of permanent dynamics. In the exceptional case that $b = 2c$, the above equation is variational. We remark that Eq. (1) is temporal and spatial translation invariant. Moreover, it is invariant under spatial reflection symmetry ($x \rightarrow -x$).

A. Spatiotemporal chaos of patterns

It is well-known that the Swift-Hohenberg equation with negative diffusion ($\nu < 0$, $b = c = 0$) exhibits stationary patterns in a wide range of parameters [4,5]. The inclusion of nonvariational terms allows the emergence of permanent dynamics behavior as equilibrium states, such as oscillations, chaos, spatiotemporal chaos, and so on [25]. In order to find the parameter region where the patterns are observed, a weakly nonlinear analysis of a critical model can be performed following the standard amplitude equation method [3,5]. This analysis reveals that the parameter c does not play a role in the transition between uniform and pattern state. Hence, c is a suitable parameter to investigate the emergence of complexity over the pattern solutions.

Numerically, we investigate the dynamics of the patterns for different values of the nonlinear advection parameter c and observe the alteration in the dynamics of the pattern state. It must be pointed out that a balance between c and b is required to sustain the permanent dynamics. In all numerical
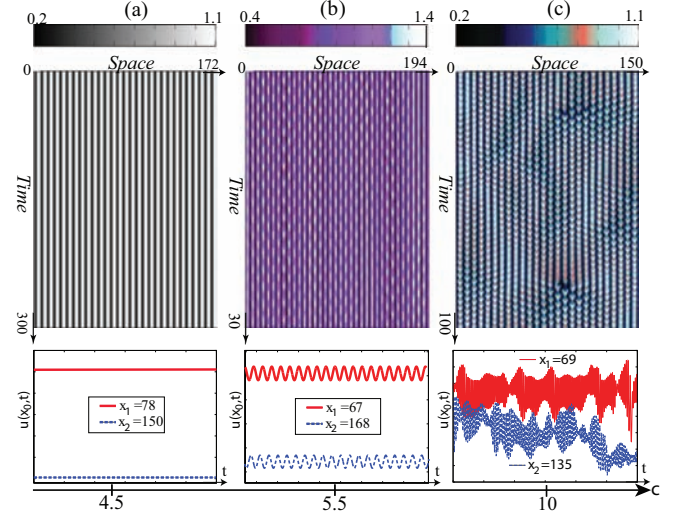

FIG. 1. (Color online) Spatiotemporal diagram of the field $u(x,t)$ observed in the nonvariational generalization of the Swift-Hohenberg model, Eq. (1), $\eta = -0.04$, $\epsilon = -0.0921$, $\nu = -1$, $b = -3.5$, with a discretization of 512 points, $dx = 0.6$, $dt = 0.01$, (a) $c = 4.5$, (b) $c = 5.5$, and (c) $c = 10$ show, respectively, stationary, oscillatory, and spatiotemporal chaotic patterns. The lower panels show the temporal evolution of two arbitrary spatial points of the respective spatiotemporal diagram.

simulations conducted along this work we use a linear Algebra library [30]. The algorithm is a scheme of finite difference for the space (with up to four neighbors) with specular boundary conditions and a fourth-order Runge-Kutta algorithm for the time evolution.

For $c < c_{AH} \equiv 5.440 \pm 0.005$, the pattern is stationary. Figure 1(a) shows a spatiotemporal diagram of the typically observed pattern. As we increase c, the pattern exhibits oscillations and complex spatiotemporal behavior as illustrated in the spatiotemporal diagram showed in Fig. (1). To illustrate the complex dynamics exhibited by the system, in the lower panels of Fig. (1), we have considered the temporal evolution of two points of the system. From this evolution, one clearly observes periodic and aperiodic dynamical behaviors. When c is large enough the system exhibits spatiotemporal chaos. In order to figure out the complex dynamics exhibited by the patterns, we consider a region of the parameter space where the spatiotemporal diagram of the field $u(x,t)$ is more complex [see Figs. 2(a) and 2(c)]. From this figure, it is easy to see that the spatiotemporal diagram is characterized by patches that exhibit large amplitude oscillations of the pattern with a complex spatiotemporal structure. Another intuitive way to understand the complex behavior exhibited by patterns is to consider two slightly different initial conditions and the auxiliary field

$$\zeta(x,t) = |u(x,t) - u'(x,t)|, \qquad (2)$$

where $u(x,t)$ and $u'(x,t)$ are the order parameter with slightly different initial conditions, and the symbol $|\cdot|$ accounts for absolute value. Thus, $\zeta(x,t)$ accounts for the evolution of the difference between two different initial conditions. Figure 2 shows the evolution of the order parameter $u(x,t)$ and the field difference $\zeta(x,t)$ with a small difference in the initial
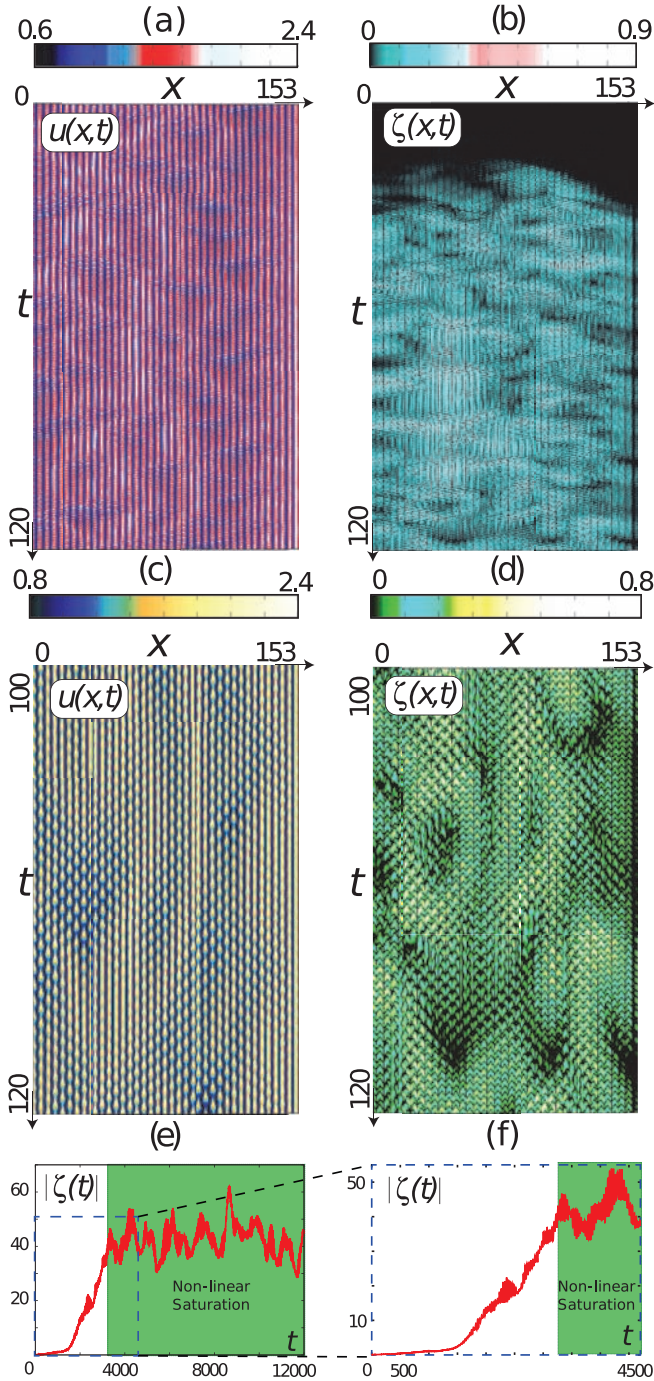
FIG. 2. (Color online) spatiotemporal dynamics of one-dimensional pattern of Eq. (1), in the parameter space $\eta = -0.04$, $\epsilon = -0.0921$, $\nu = -1$, $b = -4.0$, and $c = 10$ with a discretization of 256 points, $dx = 0.6$, $dt = 0.01$. (a) Spatiotemporal diagram of $u(x,t)$. (b) Spatiotemporal diagram of the field $\zeta(x,t)$ obtained from a small localized initial difference of order 10^{-2}. The respective spatiotemporal diagrams (c) and (d) correspond to an enlargement of the diagrams (a) and (b). The temporal evolution of the spatial norm of the difference field $|\zeta(t)|$ is defined by Eq. (3).

condition. In order to emphasize the complexity behind this spatiotemporal evolution in Figs. 2(c) and 2(d) we show a magnification of the respective space-time diagrams. In addition, we have considered the temporal evolution of the

spatial norm of the difference field

$$|\zeta(t)| = \int |\zeta(x,t)|dx. \tag{3}$$

Figures 2(e) and 2(f) illustrate the temporal evolution of this variable. The system is characterized by initially exhibited exponential growth of $|\zeta(t)|$ and subsequently shows a saturation. This is the typical dynamical behavior observed for two initial conditions in chaotic systems. From this figure we can infer that the evolution of the pattern is sensitive to initial conditions. Furthermore, the difference field $\zeta(x,t)$ has a complex spatiotemporal structure, which at different time scales has a similar spatial structure, revealing the order behind complexity.

B. Lyapunov spectrum

A characterization of chaos and spatiotemporal chaos can be done by means of Lyapunov exponents [31]. These exponents measure the growth rate of generic small perturbations around of a given trajectory in finite-dimensional dynamical systems. The Lyapunov exponents depend on the linear operator, deduced by linearizing the dynamic around the trajectory before mentioned. There are as many exponents as the dimension of the system under study. Additional information about the complexity of the system could be obtained from the exponents, for instance, the dimension of the strange attractor (spectral dimensionality) or dynamic disorder measures (entropy) [33].

The analytical study of Lyapunov exponents is a titanic endeavor and in practice inaccessible, then the logical strategy is a numerical derivation of the exponents. To study numerically the Lyapunov exponents is necessary to discretize the partial differential equation. Let N be the number of discretization points. Thus, the system has N Lyapunov exponents. We introduce the following notation for the Lyapunov exponents $\{\lambda_i\}$, where i parameterizes the numbers of points $(i = 1, \ldots, N)$. If we sort in a decreasing manner the Lyapunov exponents, when N diverges (*thermodynamic limit*) these exponents converge to a continuous spectrum as Ruelle conjectured [32]. Therefore, if the system has spatiotemporal chaos in the thermodynamic limit, there are an infinite number of positive Lyapunov exponents. That is, in extended systems, the notion of Lyapunov exponents should be generalized to a Lyapunov density $\lambda_i \to \lambda(x)$.

The set of Lyapunov exponents provides an upper limit for the strange attractor dimension through the Yorke-Kaplan dimension [33]

$$D_{\mathrm{YK}} = p + \sum_{i=1}^{p} \frac{\lambda_i}{\lambda_{p+1}}, \tag{4}$$

where p is the largest integer that satisfies $\sum_{i=1}^{p} \lambda_i > 0$. In parallel, the Kolmogorov-Sinai entropy (S_{KS}) measures the information of the system [33]. This entropy is defined as

$$S_{\mathrm{KS}} = \sum_{i=1}^{\kappa} \lambda_i > 0, \tag{5}$$

where κ is the largest integer that satisfies $\lambda_\kappa > 0$. In the thermodynamic limit the Yorke-Kaplan dimension and the

Kolmogorov-Sinai entropy diverge with the size of the system as consequence of the Lyapunov density [34].

The above properties are the main features of spatiotemporal chaos or extended chaos [6]. It is noteworthy that these properties from the point of view of experimental observations are difficult. Then, it is required to develop appropriate tools to overcome this difficulty.

We have conducted numerical simulations of Eq. (1) for different Ns and large c, in order to verify the above properties. Furthermore, we have computed partially the Lyapunov exponents, using the strategy proposed in Ref. [44]. Introducing a small perturbation $\delta u(x,t) \equiv u_s(x,t) - u(x,t)$ around a given trajectory u_s, replacing in Eq. (1) we get

$$\partial_t \delta u = \mathcal{L}(u_s)\delta u, \tag{6}$$

with the linear operator

$$\mathcal{L} \equiv \epsilon - 3u_s^2 + 2c\partial_x u_s \partial_x + b\partial_{xx} u_s + (\nu + bu_s)\,\partial_{xx} - \partial_{xxxx}.$$

The calculation numerically of the Lyapunov exponents from the above equation is a complex task, as the dominant direction suppresses the other ones. Hence, to compute the first larger $k \leqslant N$ Lyapunov exponents, we consider a discrete approximation of Eq. (1), introducing a stability parameter $\gamma > 0$, and augmenting the dynamical system with an orthonormal k-dimensional frame $\{\hat{e}_i(t)\}_{i=1}^k$. To keep the orthonormality of this base, we solve the augmented dynamical system, composed by Eq. (1) and

$$\partial_t Q = \mathcal{L}(u_s)Q - QT - \gamma Q(Q^t Q - I_k), \tag{7}$$

where Q is a matrix whose columns correspond to the vectors of the dynamical base $\{\hat{e}_i(t)\}$, Q^t accounts for the transpose of Q, I_k is a k-rank identity matrix and T is the upper-triangular matrix define by [44]

$$T_{ij} = \begin{cases} (Q^t\mathcal{L}Q)_{ij} + (Q^t\mathcal{L}Q)_{ji} & i > j, \\ (Q^t\mathcal{L}Q)_{ij} & i = j, . \\ 0 & j < i \end{cases} \tag{8}$$

As the complete system is computed, each Lyapunov exponent in the partial spectrum attains a definite value, which can be calculated as [44]

$$\lambda_i = \lim_{t \to \infty} \frac{T_{ii}}{t}. \tag{9}$$

Figure 3(a) depicts the Lyapunov spectrum obtained for different Ns and shows that the Lyapunov spectrum converges to a well-defined smooth curve (Lyapunov density), when one considers the intensive variable i/N. Hence, in the thermodynamic limit the number of positive Lyapunov exponents diverges. On the other hand, the spectral dimension D_{YK} diverges proportional to the system size, which is consistent with Ruelle conjecture (cf. Fig. 3) [31,32,34]. A similar behavior of the Lyapunov spectrum is observed in Ginzburg-Landau-type oscillators with global coupling [35,36], Kuramoto-Sivashinsky equation [31,37], Ginzburg-Landau model [38], excitable medium [39], and Boussinesq equations for Rayleigh-Benard convection [40]. Therefore, from the above numerical analysis we can conclude that the dynamical behavior exhibited by patterns in the nonvariational
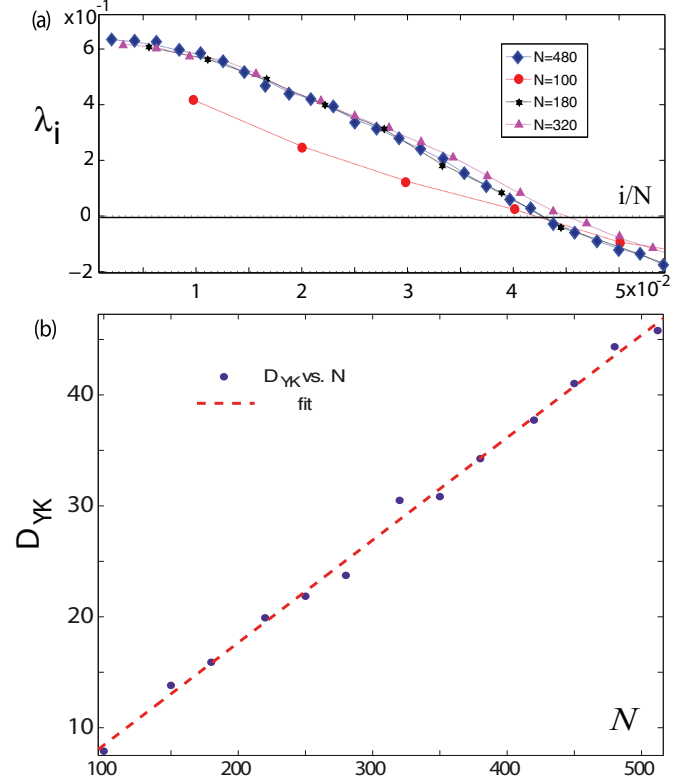

FIG. 3. (Color online) Characterization of extended chaos. (a) Lyapunov spectrum of Eq. (1) for different numbers of integration points, in the parameter space $\eta = -0.04$, $\epsilon = -0.0921$, $\nu = -1$, $b = -3.5$, and $c = 10$. (b) Yorke-Kaplan dimension as function of the number of integration points. The linear growth of the Yorke-Kaplan dimension can be fitted by a slope of 0.0924 and intersects -0.8087. The spectrum was computed using $\gamma = 160$ as stabilization value for Eq. (7).

generalization of the Swift-Hohenberg model, Eq. (1), for large c is spatiotemporally chaotic.

III. ROUTE TO SPATIOTEMPORAL CHAOS IN ONE-DIMENSIONAL PATTERN FORMING SYSTEMS

To understand the origin of the observed pattern complex dynamical behavior of Eq. (1), we use as order parameter the largest Lyapunov exponent defined by

$$\lambda_1 = \lim_{t \to \infty} \lim_{\Delta_0 \to 0} \frac{1}{t} \ln\left[\frac{||u(x,t) - u'(x,t)||}{||u(x,t_o) - u'(x,t_o)||}\right], \tag{10}$$

where $u(x,t)$ and $u'(x,t)$ are two solutions of Eq. (1), $\Delta_o \equiv ||u(x,t_0) - u'(x,t_0)||$ and $||f(x,t)||^2 \equiv \int |f(x,t)|^2 dx$ is the used norm. $\Delta(t) \equiv ||u(x,t) - u'(x,t)||$ stands for the global evolution of the difference between the fields. In order to calculate the largest Lyapunov exponent in an efficient manner, we use the strategy proposed in Ref. [41]. Which correspond to consider an orbit $u(x,t)$ and the dynamics around, characterized by Eq. (6) with a small $\delta u(x,t)$. Then we obtain the temporal evolution of $\delta u(x,t)$ and $\Delta(t)$. Assuming an exponential growth of $\Delta(t)$, the maximum Lyapunov exponent corresponds to the slope of $\log[\Delta(t)/\Delta_0]$.

When λ_1 is positive or negative, the perturbation of a given trajectory is characterized by an exponential separation or
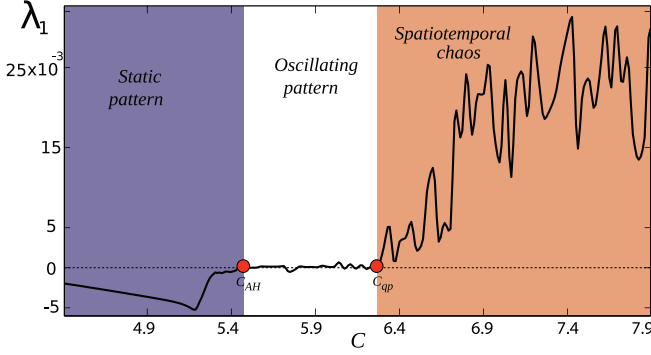
FIG. 4. (Color online) Bifurcation diagram of Eq. (1). Largest Lyapunov exponent of Eq. (1) as a function of the nonlinear advection parameter c for $\eta = -0.020$, $\epsilon = -0.092$, $\nu = -1.000$, and $b = -3.000$.

approach, respectively. Hence, attractors such as stationary patterns or uniform equilibria are characterized by negative λ_1. Conversely, complex behaviors such as chaos and spatiotemporal chaos will exhibit positive λ_1. Dynamical behaviors with zero largest Lyapunov exponent correspond to equilibria with invariant directions, such as periodic or quasiperiodic solutions and nonchaotic attractors characterized with polynomial growth rate [33].

Figure 4 shows the largest Lyapunov exponent λ_1 of the pattern state as a function of the nonlinear advection parameter c for Eq. (1). This largest Lyapunov exponent allows us to distinguish clearly three different regimes exhibited by the system. For $c < c_{AH}$, the system exhibits a stable stationary pattern. Then, we call this a region of static patterns. When c is increased and approaches $c_{AH} = 5.440 \pm 0.005$, the pattern becomes unstable (zero Lyapunov exponent) through a subcritical Andronov-Hopf bifurcation.

A. Andronov-Hopf bifurcation

In order to characterize this bifurcation, we have considered $c \lesssim c_{AH}$ and numerically determined the pattern solution of Eq. (1), $u_p(x)$ (see Fig. 5). Linearizing the dynamics around this periodic solution [cf. Eq. (6)], subsequently computing the eigenvalues of $\mathcal{L}[u_p(x)]$ operator leads us to the spectrum. However, in the continuous limit is a complex task to calculate this spectrum. Then we have considered the alternative of calculating this spectrum numerically by discretizing the system. Then $\mathcal{L}[u_p(x)]$ becomes a matrix and
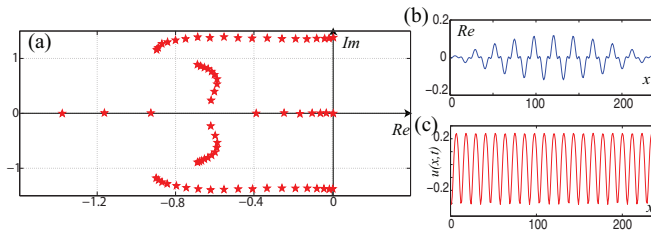

FIG. 5. (Color online) Numerical characterization of Andronov-Hopf bifurcation of Eq. (1) with specular boundary condition. (a) Sets of eigenvalues of the operator $\mathcal{L}[u_p(x)]$; (b) real part of the marginal mode; (c) periodic solution $u_p(x)$.

the eigenvalues are obtained by the diagonalization of this matrix. The respective spectrum is shown in Fig. 5(a). This spectrum shows that the pattern presents an Andronov-Hopf bifurcation, that is, two complex conjugated eigenvalues will cross the imaginary axis on the complex plane. The eigenvalue at the origin of the complex plane stands for the Goldstone mode due to the spatial translation invariance [42]. Note that the marginal mode with nonzero imaginary part is not spatially uniform and its spatial period is twice the wavelength of the stationary pattern [cf. Figs. 5(b) and 5(c)]. On the onset of the Andronov-Hopf bifurcation ($c \gtrsim c_{AH}$), the system is characterized by inhomogeneous spatial oscillations of finite amplitude, which can be decomposed as the superposition of the original pattern and the marginal critical mode with nonzero imaginary part.

Complementary information can be extracted from the power spectrum density $F(f) = \mathcal{F}(|\zeta(t)|)$ of the temporal trace of the spatial norm of the difference field $|\zeta(t)|$ [see Eq. (3)]. Figure 6 shows the $F(f)$ of $|\zeta(t)|$ and the spatiotemporal diagram of $u(x,t)$ for different parameters. The power spectrum density can be used to understand how the excited spatiotemporal modes evolve and interact. We note that the dynamics exhibited by the system, when $c \gtrsim c_{AH}$, is dominated by the fundamental frequency and its harmonics (see left-hand inset in Fig. 6). It is important to note that an extended system that displays an Andronov-Hopf bifurcation can exhibit generically spatiotemporal chaotic behavior [21,43].

Close to the Andronov-Hopf bifurcation, we can introduce the ansatz

$$u(x,t) = u_p[x - x_o(x,t),t] + A(x,t)e^{i\omega t}u_{2p}(x - x_o) + \text{h.o.t}, \tag{11}$$

where $u_p(x,t)$ stands for the stationary pattern with spatial period p, which undergoes the Andronov-Hopf bifurcation [cf. Fig. 5(c)] and $u_{2p}(x)$ stands for the critical marginal mode with spatial period $2p$ and frequency ω [cf. Fig. 5(b)], $x_o(x,t)$ stands for the dynamical evolution of the spatially invariant translational mode, A stands for the amplitude of u_{2p} and h.o.t are higher order terms. Following Ref. [42], A satisfies a subcritical complex Ginzburg-Landau equation, when the cycle of bistability is small; i.e., in the previous ansatz it makes sense to consider the amplitude small [$A(x,t) \ll 1$] [31]. However, the bistability cycle shown by Eq. (1) does not have a region where A is small. Figure 7 shows the typical bistability cycle observed in this system. From this figure we can infer that the oscillatory solution appears through a subcritical bifurcation of a large amplitude, also it exhibits a secondary bifurcation, which corresponds to another oscillatory solution. Due to the large hysteresis loop and the secondary instability of the bifurcated state, the subcritical complex Ginzburg-Landau equation only describes qualitatively the dynamics around c_{AH}.

Hence, in the second region identified on the bifurcation diagram presented in Figs. 4 and 6, $c_{AH} < c < c_{QP} \equiv 6.350 \pm 0.005$ the dynamic of the pattern does not change qualitatively. The pattern exhibits localized oscillations dominated by just one frequency and its harmonics (see left panel of Fig. 6). This parameter region displays a plateau in the largest Lyapunov exponent (see the intermediate region illustrated in Figs. 4 and 6). We have named this region as the *oscillating pattern*
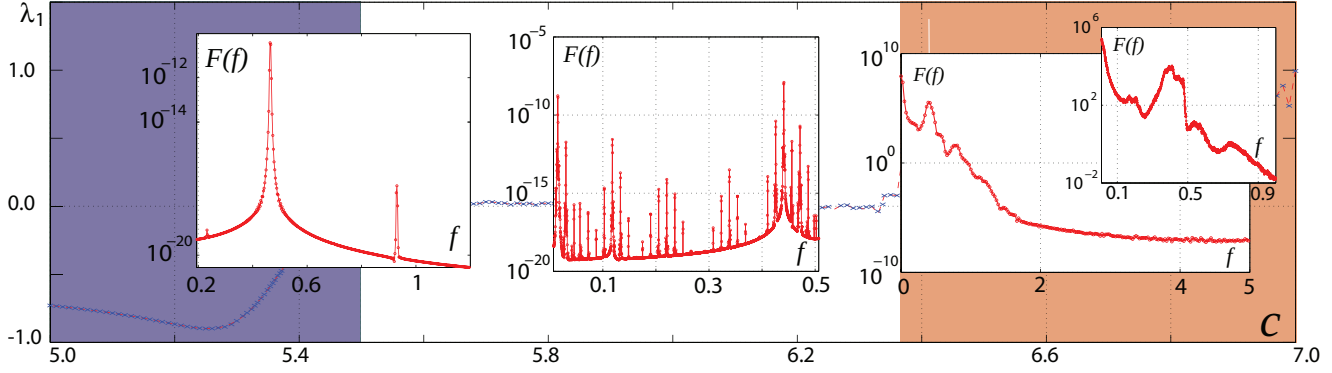
FIG. 6. (Color online) Spatiotemporal quasiperiodicity route for pattern of Eq. (1) as a function of nonlinear advection c with $\eta = -0.020$, $\epsilon = -0.092$, $v = -1.000$, and $b = -3.000$. We show in the respective regions the typically observed frequency power spectrum $F(f)$ of the evolution of the spatial norm of the difference field $|\zeta(t)|$ using acquisition frequency 0.1.

zone. It is important to note that the frequency power spectrum, $F(f)$, of the evolution of the $|\zeta(t)|$ throughout this region has a similar shape, that is, the $F(f)$ is governed by the Andronov-Hopf frequency of patterns and its harmonics.

B. Emergence of spatiotemporal chaos

When c exceeds c_{QP}, the largest Lyapunov exponent exhibits a qualitative change in its behavior. λ_1 starts to increase as shown in Fig. 4 and becomes positive. Spatiotemporal diagrams in this region exhibit spatiotemporal chaos, as illustrated in Figs. 1 and 2. In order to understand the origin of this complex behavior, for $c_{QP} \lesssim c$, we calculate the frequency power spectrum $F(f)$ of the $|\zeta(t)|$ and we observe the emergence of a new incommensurable frequency (see inset on the center Fig 6). Later, the discrete $F(f)$ changes

toward a continuous power density spectrum (see curve in the inset on the right-hand side in Fig 6). Figure 4 illustrates the region where spatiotemporal chaos of patterns is observed. We have named this region as *spatiotemporal chaos zone*. Notice that throughout this region ($c > c_{QP}$) the frequency power spectrum is qualitatively similar. The frequency power spectrum allows us to conclude that the appearance of this incommensurable second frequency is responsible for the destabilization of the patterns oscillation and for the emergence of complex spatiotemporal behavior for the pattern.

To understand the origin of the emergence of a quasiperiodical behavior, we have studied numerically the evolution of the five larger Lyapunov exponents around the transition points. Figure 8 shows the evolution of these Lyapunov exponents as a function of the nonlinear advection parameter c. From this figure we can infer that the appearance of the second frequency is associated with the second larger Lyapunov exponent crossing the horizontal axis and then it is followed by the other Lyapunov exponents. Around this transition region a relevant number of Lyapunov exponents are positive, then one expects the emergence of spatiotemporal chaos.
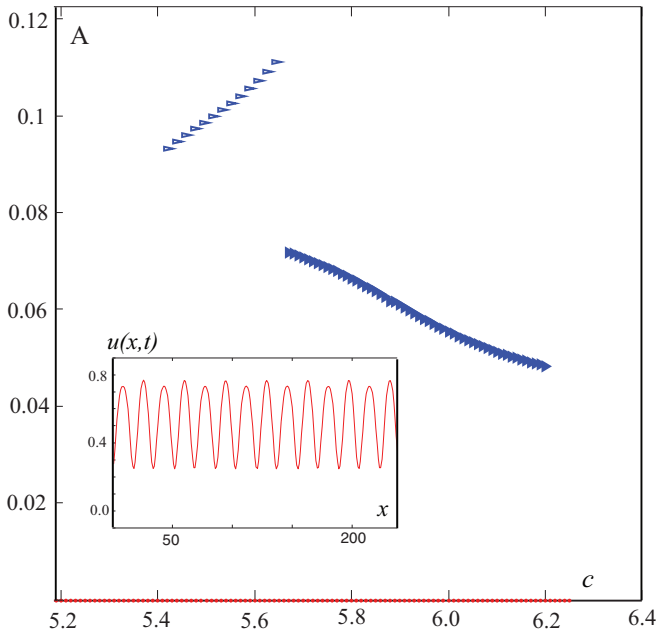

FIG. 7. (Color online) Hysteresis loop of the bifurcated solutions of Eq. (1) with $\eta = -0.020$, $\epsilon = -0.092$, $v = -1.000$, and $b = -3.000$. A stands for the modulus of the amplitude of the critical marginal mode with spatial period $u_{2p}(x)$.
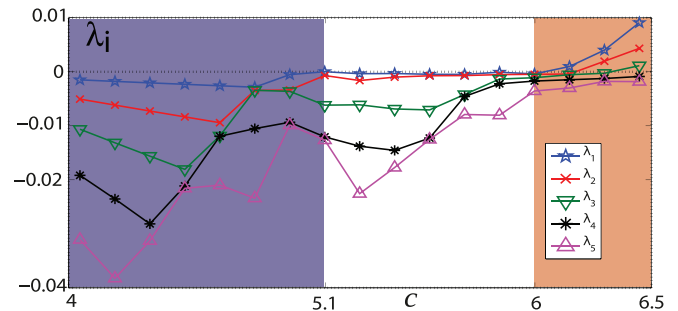

FIG. 8. (Color online) Five largest Lyapunov exponents as functions of the nonlinear advection parameter c. The colored areas represent the different regions of dynamic behaviors. The static pattern region is characterized by having only negative Lyapunov exponents. The oscillatory pattern region presents a plateau and its largest Lyapunov exponent is zero. Finally, the region of chaotic spatiotemporal pattern is characterized by the crossing of the horizontal axis by its Lyapunov exponents and thus becoming positive.

In brief, the exhibited dynamical behavior of the Lifshitz normal form, Eq. (1), is a natural extension of the quasiperiodicity route for low-dimensional chaos of limit cycles [22] to patterns in extended systems.

IV. CONCLUSION AND REMARKS

In modern dynamical systems theory there are two milestones, the theory of turbulence by A. Kolmogorov in 1941 [45] and the rediscovery of chaos by hands of the meteorologist E. Lorenz in 1963 [46]. These two milestones can be seen as two limits in the description of complexity. Low dimensional chaotic behavior could be obtained by a system with, at least, three degrees of freedom; on the other hand, turbulence needs infinite degrees of freedom in their description. In this framework, spatiotemporal chaos is a dynamical behavior of a system that needs infinite degrees of freedom; however, it does not obey the statistical rules required by the turbulence theory. To date, the study of spatiotemporal chaos in an extended system is still, in general, an open and fundamental question.

Following the pioneering line of thought that Landau used to understand turbulence [47], this intricate dynamical behavior must be a result of a sequence of instabilities. We have considered a universal model that describes patterns formation, where by modifying a single parameter, a transition from a steady pattern toward a spatiotemporal chaotic behavior appears. The signature of this route is an Andronov-Hopf bifurcation of the stationary pattern accompanied by the emergence of an oscillatory pattern, to be then replaced by the final spatiotemporal chaotic pattern as a second incommensurate frequency develops. The exhibited dynamical behavior is a natural extension of the quasiperiodicity route of low-dimensional chaos to extended systems.

A Similar route has been observed for traveling waves at the onset of spatiotemporal chaos in a wide class of Galilean invariant models [8]. This similarity is a consequence of the fact that primary bifurcations such as Andronov-Hopf are of low dimension. That is, the number of unstable modes is small. Contrarily, secondary bifurcations are characterized by a large number of modes becoming unstable simultaneously. This property is shown in the large number of Lyapunov exponents that become positive.

The presented scenarios for spatiotemporal chaos in one-dimensional pattern-forming systems have been characterized by the larger Lyapunov exponents and spatiotemporal chaos by its respective Lyapunov density. The largest Lyapunov exponent is an appropriate order parameter to characterize emergence of complex dynamical behaviors such as spatiotemporal chaos. The strategy presented can be implemented in any extended dynamic system, which exhibits the emergence of complex spatiotemporal behavior, where tools such as Lyapunov density play a central role in the characterization of complexity.

The nonvariational generalization of the Swift-Hohenberg model, Eq. (1), besides exhibiting spatiotemporal chaos also presents coexistence with uniform state. Then, this model exhibit localized complex state [16] or fronts between these states. These interfaces show intricate dynamic behavior, studies on the characterization of this type of dynamics are in progress.

[1] P. Ball, *The Self-Made Tapestry: Pattern Formation in Nature* (Oxford University Press, New York, 1999).

[2] G. Nicolis and I. Prigogine, *Self-Organization in Non Equilibrium Systems* (J. Wiley & Sons, New York, 1977).

[3] L. M. Pismen, *Patterns and Interfaces in Dissipative Dynamics* (Springer Series in Synergetics, Berlin/Heidelberg, 2006).

[4] M. Cross and H. Greenside, *Pattern Formation and Dynamics in Nonequilibrium Systems*, (Cambridge University Press, New York, 2009).

[5] M. C. Cross and P. C. Hohenberg, Rev. Mod. Phys. **65**, 851 (1993).

[6] G. Nicolis, *Introduction to Nonlinear Science* (Cambridge University Press, Cambridge, 1995).

[7] P. Coullet and J. Lega, Europhys. Lett. **7**, 511 (1988); P. Coullet, L. Gil, and J. Lega, Phys. Rev. Lett. **62**, 1619 (1989); Physica D **37**, 91 (1989).

[8] G. Goren, J. P. Eckmann, and I. Procaccia, Phys. Rev. E **57**, 4106 (1998).

[9] W. Decker, W. Pesch, and A. Weber, Phys. Rev. Lett. **73**, 648 (1994); B. Echebarria and H. Riecke, *ibid.* **84**, 4838 (2000); K. E. Daniels and E. Bodenschatz, *ibid.* **88**, 034501 (2002).

[10] M. A. Miranda and J. Burguete, Phys. Rev. E **79**, 046201 (2009).

[11] P. Brunet and L. Limat, Phys. Rev. E **70**, 046207 (2004).

[12] Q. Ouyang and J. M. Flesselles, Nature (London) **379**, 143 (1996).

[13] Z. Qu, J. N. Weiss, and A. Garfinkel, Phys. Rev. Lett. **78**, 1387 (1997).

[14] S. Q. Zhou and G. Ahlers, Phys. Rev. E **74**, 046212 (2006).

[15] S. J. Moon, M. D. Shattuck, C. Bizon, D. I. Goldman, J. B. Swift, and H. L. Swinney, Phys. Rev. E **65**, 011301 (2001).

[16] N. Verschueren, U. Bortolozzo, M. G. Clerc, and S. Residori, Phys. Rev. Lett. **110**, 104101 (2013).

[17] H. Chate, Nolinearity **7**, 185 (1994).

[18] F. Brochard, E. Gravier, and G. Bonhomme, Phys. Rev. E **73**, 036403 (2006).

[19] E. L. Rempel and Abraham C.-L. Chian, Phys. Rev. Lett. **98**, 014101 (2007); K. He and Abraham C.-L. Chian, Phys. Rev. E **69**, 026207 (2004); K. He, Phys. Rev. Lett. **80**, 696 (1998).

[20] J. A. Sherratt and M. J. Smith, Physica. D **241**, 1671 (2012).

[21] Yoshiki Kuramoto, *Chemical Oscillations, Waves, and Turbulence* (Springer, New York, 1984).

[22] D. Ruelle and F. Takens, Commun. Math. Phys. **20**, 167 (1971).

[23] P. Berge, Y. Pomeau, and C. Vidal, *Order within Chaos: Towards a Deterministic Approach to Turbulence* (John Wiley & Sons, New York, 1984).

[24] J. Swift and P. C. Hohenberg, Phys. Rev. A **15**, 319 (1977).

[25] S. Residori, A. Petrossian, T. Nagaya, and M. G. Clerc, J. Opt. B: Quantum Semiclassical Opt. **6**, S169 (2004); M. G. Clerc, A. Petrossian, and S. Residori, Phys. Rev. E **71**, 015205(R) (2005).

[26] G. Kozyreff, S. J. Chapman, and M. Tlidi, Phys. Rev. E **68**, 015201 (2003)

[27] C. Durniak, M. Taki, M. Tlidi, P.-L. Ramazza, U. Bortolozzo, and G. Kozyreff, Phys. Rev. E **72**, 026607 (2005).

[28] G. Kozyreff and M. Tlidi, Chaos **17**, 037103 (2007).

[29] A. C. Newell, T. Passot, and J. Lega, Ann. Rev. Fluid Mech. **25**, 399 (1993).

[30] Conrad Sanderson, *Armadillo: An Open Source C++ Linear Algebra Library for Fast Prototyping and Computationally Intensive Experiments*. Technical Report, NICTA (2010).

[31] P. Manneville, *Dissipative Structures and Weak Turbulence* (Academic Press, San Diego, 1990).

[32] D. Ruelle, Commun. Math. Phys. **87**, 287 (1982).

[33] E. Ott, *Chaos in Dynamical Systems*, 2nd ed. (Cambridge University Press, Cambridge, 2002).

[34] M. R. Paul, M. I. Einarsson, P. F. Fischer, and M. C. Cross, Phys. Rev. E **75**, 045203 (2007).

[35] N. Nakagawa and Y. Kuramoto, Physica. D **80**, 307 (1995).

[36] V. Hakim and W. J. Rappel, Phys. Rev. A **46**, R7347 (1992).

[37] P. Manneville, *Lecture Notes in Physics*, Vol. 280 (Springer, Berlin, 1994), pp. 319–326.

[38] D. A. Egolf and H. S. Greenside, Nature **369**, 129 (1994).

[39] M. C. Strain and H. S. Greenside, Phys. Rev. Lett. **80**, 2306 (1998).

[40] D. A. Egolf, I. V. Melnikov, W. Pesch, and R. E. Ecke, Nature **404**, 733 (2000).

[41] R. Deissler and K. Kaneko, Phys. Lett. A **119**, 397 (1987).

[42] P. Coullet and G. Iooss, Phys. Rev. Lett. **64**, 866 (1990).

[43] I. Aranson and L. Kramer, Rev. Mod. Phys. **74**, 99 (2002).

[44] F. Christianen and H. H. Rough, Nonlinearity **10**, 1063 (1997); T. J. Bridges and S. Reich, Physica D **156**, 219 (2001).

[45] U. Frisch, *Turbulence: The Legacy of A. N. Kolmogorov* (Cambridge University Press, Cambridge, 1995).

[46] E. N. Lorenz, J. Atmos. Sci. **20**, 130 (1963).

[47] L. Landau, C. R. Acad. Sci. USSR **44**, 311 (1944).